



Synthesis, characterization, molecular docking and antibacterial activities of Bis-[(E)-3{2-(1-4-chlorophenyl) ethylidene}hydrazinyl]-N-(4-methylphenyl)-3-oxopropanamideZinc (II) complex

Richa Kothari^{1*}, Anurag Agrawal² & Sanchita Rai¹

¹Department of Chemistry, School of Science; & ²School of Pharmacy, ITM University, Gwalior-474 005, Madhya Pradesh, India

Received 04 October 2020; revised 28 June 2021

The title Zn (II) complex was synthesized by reacting the compound Bis-[(E)-3{2-(1-4-chlorophenyl) ethylidene}hydrazinyl]-N-(4-methylphenyl)-3-oxo propanamide with Zn (II) chloride dihydrate in alkaline dimethylsulphoxide and ethanol solution under refluxing condition for 8 h. The resultant compound was filtered and recrystallized from ethanol. The hydrazone Schiff base ligand and its Zn (II) complex were characterized by using UV-Vis spectroscopy and XRD, TEM and SEM analysis. The antibacterial activities of ligand and its Zn complex were examined using disc diffusion method. The spectra results showed that the hydrazone ligand undergoes keto-enol tautomerism forming a bidentate ligand (N,N) towards Zn⁺² (II) ion. It is very interesting that on sides of the two hydrazone ligands which coordinate to the Zn⁺² ions, an additional two thiosemicarbazone moiety were also coordinated with Zn⁺² ions in the crystalline powder, resulting in a hexa coordinated octahedral Zn (II) complex. Both hydrazone Schiff base ligand and its Zn (II) complex were found to exhibit good antibacterial activity even when the concentrations were high. Molecular docking analysis also deciphered that Zinc complex and carbohydrazone ligand both were found to be fitted into the active sites of molecular targets and Zn complex showed better binding affinities towards macromolecules compared to ligand.

Keywords: Antibacterial activity, Hydrazones, Molecular docking, XRD, Zinc (II) complex

Carbohydrazone Schiff base ligand plays an important role in inorganic chemistry stream because it can readily form stable complexes with a large number of transition metal ions like Cu⁺², Fe⁺², Ni⁺², Co⁺² etc., due to its flexibility to form keto-enol tautomerism¹⁻⁴ (Fig. 1). In coordination compounds the hydrazone Schiff base ligand normally exists in enol form in order to bind with the metal ions through the nitrogen atom from imine group⁵⁻⁷ and oxygen from hydroxyl group⁸⁻⁹. Zn (II) metal ions generally have 4- coordination number and predict a tetrahedral geometry for Zinc complexes. Because Zn has completely filled d-orbitals with ten electrons and forms a stable eighteen electrons complex can be formed through four coordination numbers with Schiff base ligands. Due to this reason, 5-6 coordinate Zn complex is considered unusual and expected to be unstable in nature. However, 5-6 coordinate Zn complex were previously reported¹⁰⁻¹⁴. The oxidation state of Zn⁺² ion in Zn complex is +2. However one reported by Song *et al.* is in the zero

oxidation state. In this paper synthesis, characterization, molecular structure of Zn complex is reported. In addition, antibacterial activities and molecular docking studies of Zn complex and Carbohydrazone Schiff base have also been evaluated.

Material & Methods

Instrumentation

The IR Spectra of hydrazone Schiff base ligand L₁ and the Zn(II) complex were recorded in KBr disks by using Perkin Elmer FT-IR spectrophotometer with the wavelength range from 400 to 4000 cm⁻¹. Perkin Elmer UV/Vis lambda 25 UV-Visible spectrophotometer was used to record the electronic absorption spectra with Dichloromethane solvent. The elemental analysis of L₁ and its Zn(II) complex was conducted by using CHN Analyser, Thermo Flash EA1112 series at the temperature upto 900°C and V₂O₅ used as oxidizer to prevent inhibition caused by sulphur (Table 1). X-ray measurements for the ligand and its Zn complex were performed on a Bruker axis D8 using Cu-K α radiation ($\lambda = 1.540 \text{ \AA}$) over a 2 θ collection range of 20-80°C.

*Correspondence:
E-mail: richakothari70@gmail.com

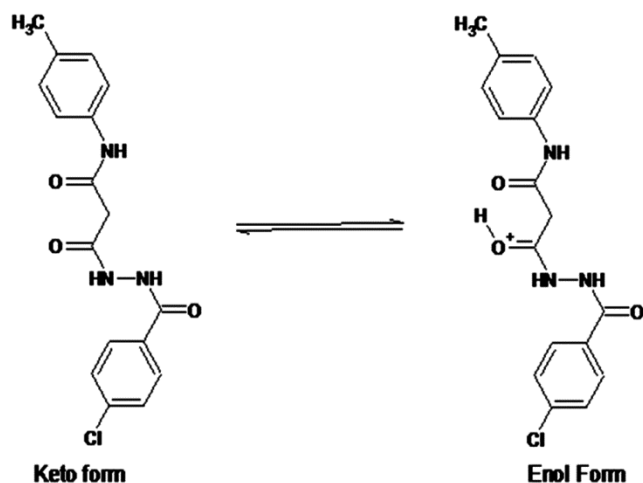


Fig.1 — Keto-enol tautomerization of a carbohydrazone Schiff base ligand

Table 1 — Spectrum: test 5165

Element(3 Sigma)	Series	unn. C [wt.%]	Norm. C [wt.%]	Atom. C [at.%]	Error [wt.%]
Carbon	K-series	45.92	59.96	73.48	27.73
Oxygen	K-series	16.74	21.86	20.11	14.29
Sulfur	K-series	2.46	3.21	1.47	0.54
Calcium	K-series	4.37	5.71	2.10	0.85
Chlorine	K-series	3.04	3.98	1.65	0.63
Zinc	K-series	4.04	5.28	1.19	2.00
Total:		76.58	100.00	100.00e	

Chemicals

All the chemicals like Zinc chloride dehydrate ($\text{ZnCl}_2 \cdot 2\text{H}_2\text{O}$), p-chloroacetophenone, Thiosemicarbazide, 4-methyl aniline, diethylmalonate, ethanol ($\text{C}_2\text{H}_5\text{OH}$) were purchased AR grade from Merck Pvt. India and were used as it is.

Synthesis

Ligand(L) and its Zn(II) complex were prepared in four stages

- (i) Synthesis of Ester
- (ii) Synthesis of hydrazide
- (iii) Synthesis of hydrazine Schiff base ligand (L)
- (iv) Synthesis of Zn(II) complex using template route.

Synthesis of Ester

In the first stage, ligand(L) was prepared using refluxing method. 4-methyl aniline, diethylmalonate and ethanol were used for synthesis of ligand 0.05 M of 4-methyl aniline is added in 10 mL of diethylmalonate. The solution is stirred continuous for 30 min at 50°C . In another beaker, we have taken 30 mL ethanol and stirred for 15 min. Then both the solution mix together and refluxed for 70°C

temperature for 1/2 h. Cool the solution and poured into solid ice. A transparent precipitate was obtained. The precipitate was obtained after 24 h aging process.

Synthesis of hydrazide

In the second stage hydrazine hydrate was used for synthesis of hydrazide 0.05 M of Ester is mixed with 0.05 M of hydrazine hydrate and stirred the solution continuously for one h at 80°C temperature. A colourless precipitate was obtained after 24 h of aging process.

Synthesis of Ligand (L)

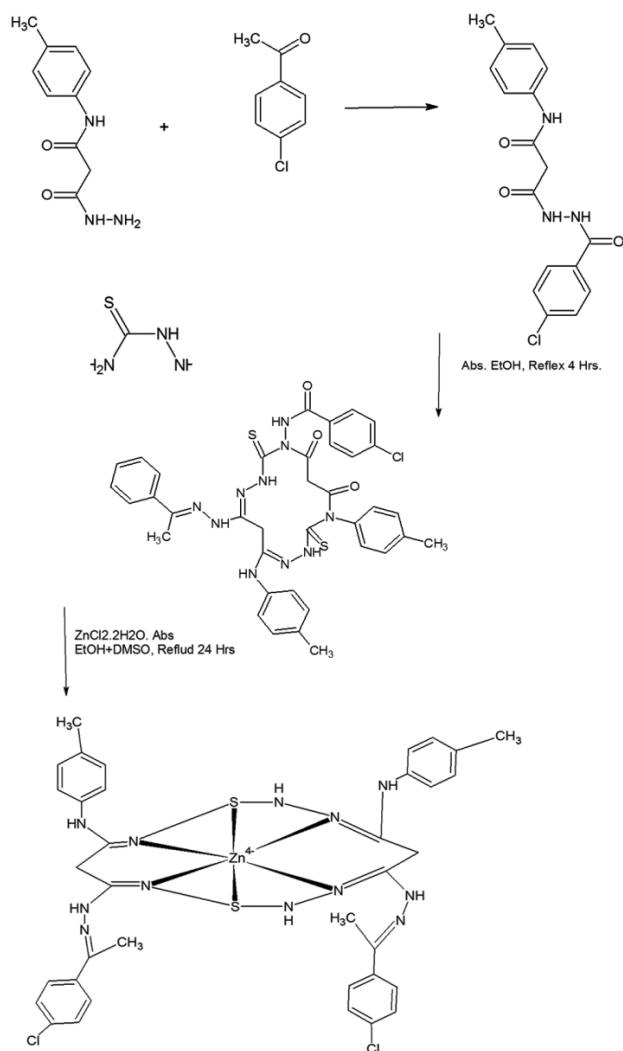
In the third stage, 1 mM of hydrazide dissolved in 50 mL ethanol and mixed with ethanolic solution of 1 mM thiosemicarbazide hydrochloride and 1 mM hydrochloride solution and stirred the solution continuously for 4 h at 80°C temperature. A white precipitate was obtained after 36 h of aging process.

Yield- 2.20 g (75.6%) and m.pt.: $215-220^\circ\text{C}$. Analytical calculation for $\text{C}_{38}\text{H}_{37}\text{N}_{14}\text{S}_2\text{Cl}_2$: C, 67.06; H, 5.47; N, 8.76; S, 10.12, Cl, 17; Found(%): C, 67.50; H, 5.68; N, 8.92; S, 11.11, Cl, 17.96. Characteristic IR absorption peaks are (KBr disk, cm^{-1}): 3435(s), 3272(s), 1610(s), 962 (m). ^1H NMR [DMSO- d_6 , δ]: 11.61 [s, 1Hz, N-H], 11.26 [s, 1 Hz, Ar-OH], 7.66 [d, 1Hz, J= 8 Hz, Ar- H], 6.96 [m, 4Hz, Ar-H], 3.41 [s, 3Hz, CH_3]. ^{13}C NMR [CD_2Cl_2 , δ]: 170.32, 163.28, 162.42, 160.86, 133.28, 130.49, 128.99, 128.60, 118.46, 117.36, 117.08, 114.86, 54.04, 41.44, 18.64. UV-Vis [DCM, λ_{max}]: 320 nM.

Synthesis of Zn (II) complex

In the fourth stage, 1 mM of hydrazone dissolved in 50 mL ethanol and stirred the solution continuously for 1/2 h at room temperature and slowly added 1 mM Zinc chloride dehydrate salt as a source of Zn^{2+} ion along with continuous stirring. The precipitate was ultrasonicated for 2 h at 80°C temperature. After 24 h aging precipitate obtains. After being refluxed for 24 h the solution was cooled to room temperature followed by filtration and recrystallization from the mixture of DMSO and absolute ethanol. A yellow coloured crystal was obtained. After one week, which was then filtered and washed with DMSO (Scheme 1).

Yield: 0.18 g (92.10%) and m.p.: $285.5-220^\circ\text{C}$. Analytical calculation for $\text{Zn}(\text{C}_{38}\text{H}_{37}\text{N}_{14}\text{S}_2\text{Cl}_2)$: C, 57.61; H, 5.14; N, 7.89; S, 10.16, Cl, 17.36; Found(%): C, 57.78; H, 5.26; N, 8.12; S, 11.28, Cl, 17.90. Characteristic IR absorption peaks are (KBr disk, cm^{-1}): 3446(s), 1620(s), 962 (m), 994(w), 660(m). ^1H NMR [CD_2Cl_2 , δ]: 8.10 [Cl, 1H, J=6.1 Hz, Ar-H], 6.92 [d & t, 2H, J=7 Hz, Ar-H], 6.72 [d, 2H, J= 9 Hz,



Scheme 1 — Synthetic Pathway of Ligand (L) and its hexa coordinate Zn (II) Complex

Ar- H], 6.96 [d & t, 2H, J = 7 Hz, Ar-H], 6.74 [d , 2H, J = 9 Hz, Ar-H], 3.66 [s, CH₃ , 3H]. ¹³CNMR [CD₂Cl₂, δ]: 172.36, 164.88, 162.20, 160.58, 133.20, 130.49, 129.86, 128.50, 118.89, 117.39, 117.40, 114.39, 54.06, 44.46. UV-Vis [DCM, λ_{max}]: 345 nM.

Molecular docking studies

In this research work, antibacterial activities were evaluated on two microorganisms *i.e.* *E. coli* and *S. aureus*, therefore crystal structures of molecular targets *i.e.* DNA gyrase subunit b (PDB ID: 1KZN) and topoisomerase II (PDB ID: 1JIJ) related to microbial potential of those mentioned microorganisms were retrieved from protein data bank. Before performing the molecular docking study, molecular targets were refined (removal of native ligands and water atoms). Macromolecules processed further into the AutoDock

execution window and saved as target .pdbqt after adding hydrogens and charges were automatically assigned on the macromolecules. Zn complex and ligand were prepared through ChemDraw Ultra 8.0 and optimized for energy minimization using MM2 force field and converted into .pdb format by OpenBabel -2.3.2 software. The Zn complex and ligand were also processed into AutoDock execution window and their torsions along with rotatable bonds are assigned and the files are saved as Zn complex .pdbqt and ligand .pdbqt, respectively. The binding modes of zinc complex and ligand with targets were obtained via AutoDock Vina software and blind docking was carried out to identify actual binding modes of zinc complex and ligand in the targets. The nine different conformers were fabricated of Zn complex and ligand and conformers which showed lowest binding energy and better interactions with molecular targets were discussed. In case of topoisomerase II, The docking parameters were defined as coordinates of the center of binding site with $x = -10.686$, $y = 20.282$, $z = 91.742$ and in case of DNA gyrase, the docking parameters were $x = 20.538$, $y = 19.166$, $z = 43.283$ and binding radius = 1.000 Å and The grid dimension used for all the three (3) proteins are $47.25 \times 47.25 \times 47.25$ Å (grid size) with point separated by 1.000 Å (grid-point spacing).

Antibacterial study of the compounds

The antibacterial study was carried out on hydrazone ligand L and its Zn(II) complex using disc two diffusion method¹⁷. One colony of each *E. Coli* (MTCC-1687), *E. faecalis* (MTCC-439), *S. aureus* (MTCC-737) and indigenous methicillin resistant *S. aureus* from a streak plate was inoculated in 20 mL of LB broth after 16 h of incubation, the optical density of the inoculums were measured and further diluted to achieve McFarland standard of 0.5 using sterile cotton swab, again plates were uniformly swabbed with diluted inoculums of bacterial cultures. After that sterile filter paper (6 mM) which were impregnated with different concentration. (*i.e.* 50, 25, 12.5, 6.25 and 3.125 μg/μL using dichloromethane as the solvent) of ligand (L₁) and its Zn(II) complex were placed the again. The inhibitory zones in millimetres were measured after 24 h of incubation. All the antibacterial assays were performing in triplicates.

Results and Discussion

Synthesis and characterisations of ligand and its Zn(II) complex

Hydrazone ligand (L) was successfully synthesised through condensation process between hydrazide and

4- chloroacetophenone under reflux for 24 h at 80°C. The colour remained unchanged even after the addition of hot ethanolic hydrazide into ethanolic solution of 4- chloroacetophenone with stirring and heating. A colourless precipitate started to form after 12 h of refluxing with the yield of 75%. The synthesized ligand L was then reacted with Zn(II) chloride under reflux condition for 28 h. Upon completion of the reaction the dark yellow solution was filtered as Pale yellow crystal after 2-3 weeks.

Based on the IR spectra of ligand (L) and its Zn(II) complex the absence of ν (N-H) and ν (C=O) peak in the IR spectrum of Zn(II) complex indicates enolization of Keto group in Ligand, which coordinate to the Zn metal ion through azomethine nitrogen atoms. The changes of frequency of IR spectra of ν (C=N), chemical shift from 1606 to 1608 cm^{-1} were rather insignificant after the complexation process. This result of the IR spectra is equivalent to the finding from Tay *et al.*¹⁵ where the IR frequency of C=N was also shifted by only 2 cm^{-1} from 1621 cm^{-1} to 1619 cm^{-1} after their ligand bis-2'-hydroxy Schiff base compound bound to Zn^{2+} ion. The IR spectral data of ligand and its Zn(II) complex is supported by the UV-Vis results where the $n \rightarrow \pi^*$ transition in C=N bond shifted from 325 to 345 nm after binding to the Zn^{2+} ion. The bathochromic shift was aroused due to the backbonding from Zn metal ion to the C=N bond in ligand and subsequently weakened the bond energy of C=N (Fig. 2).

The ^1H NMR spectra of Zn(II) complex also shows some differences compared to ligand (L_1). A broad HNMR signal at 11.82 ppm and a singlet present at 11.26 ppm of ligand L_1 are assigned to the N-H of azomethine and phenolic proton present in Schiff base ligand, respectively. These two HNMR signals showed that ligand is present in KETO form. This is also supported by the IR spectra of Schiff base ligand L_1 with the presence of ν (N-H) and ν (C=O) at 3272

and 1606 cm^{-1} , respectively. The two NMR signals at 11.82 and 11.30 ppm disappeared after complexation with Zn^{2+} ion, indicating that the structure of ligand shows Keto-enolisomerization and the N of the ligand has bound to the Zn^{2+} ion.

X-ray diffraction is a popular analytical technique which has been used for the analysis of test molecular and crystal structures. Samples were readily synthesized in alcoholic solution. Figures 3 & 4 show the XRD pattern of ligand and its zinc complex powder

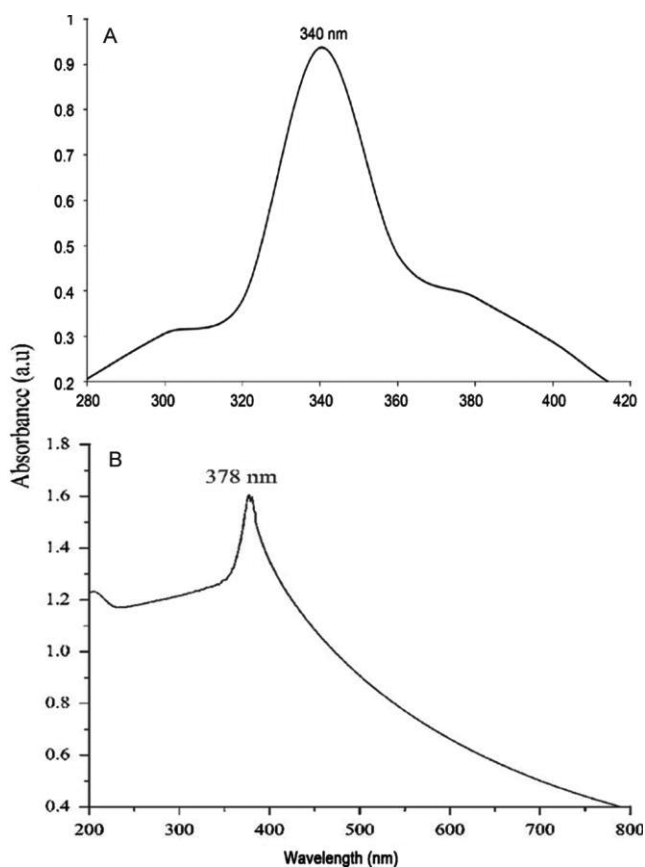


Fig. 2 — UV- Visible spectra of (A) Ligand (L); and (B) Zinc(II) complex

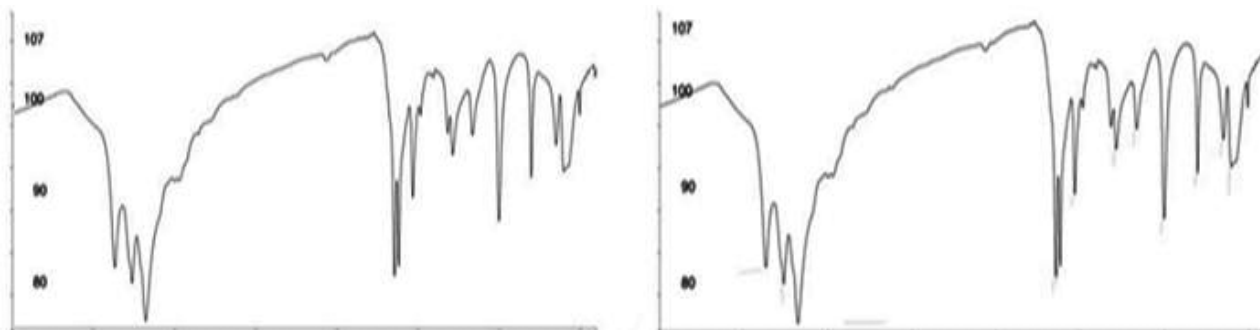


Fig.3 — FT-IR Spectra of ligand and its synthesized Zinc (II) complex

deposited from the alcoholic solution, which is in agreement with that of the standard powder diffraction of compounds with a hexagonal structure (Fig. 5). The diffraction lines are indexed as its zinc complex as 101, 102, 103, 110 phases [JCPDSNO-06-04] From the full width at half maximum of diffraction peaks (111) is employed to calculate the average crystalline size using Debye- Scherer's equation *i.e.*:

$$D = 0.9 \times \frac{\lambda}{\beta \cdot \cos \theta}$$

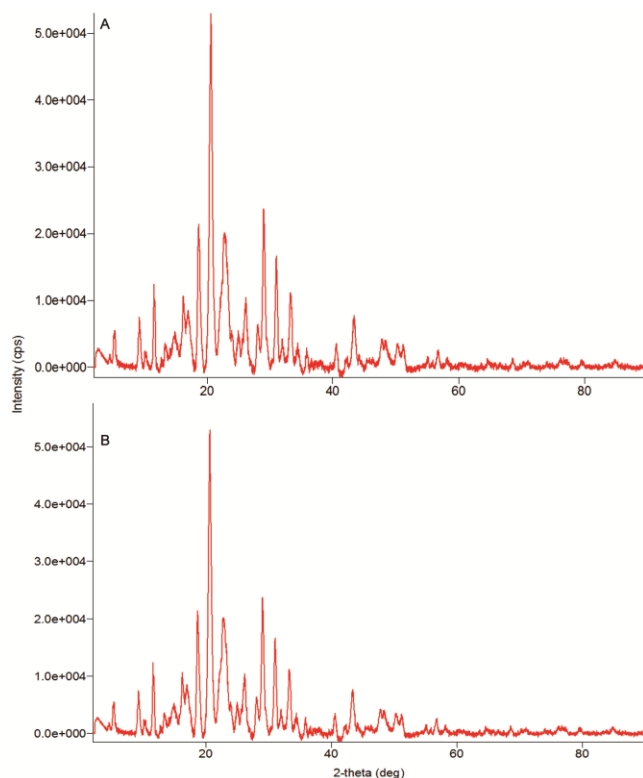


Fig.4 — XRD Spectra of Ligand and its Zinc (II) Complex

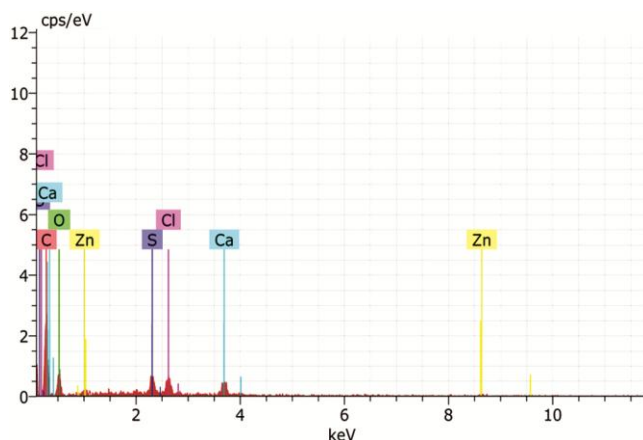


Fig.5 — EDX spectra of Zinc Complex which shows the presence of Zn, S, C, O Elements

Where,

D=Crystalline size

λ =wavelength of X-Rays

β =Full width at half maximum of the diffraction peak

θ =Bragg's angle

The estimated particle size was below 100 nM (Calculated by using Debye Scherer equation) the width of the peaks obtained in XRD pattern is cognate to the crystalline size of the particle. The small size of nanoparticles indicated the high surface area and high surface area to volume ratio¹⁵.

The estimated particle size was below 100 nM, the wider of the peaks obtained in XRD pattern is cognate to the crystalline size of zinc complex. The small size of complex indicated the high surface area to volume ratio.

EDX studies confirm the presence of zinc & sulphur elements in complex. The other impurities are found such as carbon & oxygen were identified because of the interaction with the leaf extract during bioprocessing process (Fig. 6A).

TEM images of Zinc(II) complex

The TEM images of the zinc complex are shown in (Fig. 6B). According to the picture, light coloured zinc complex is arranged in a cluster form, approximately 100 nM in size, which is expected to the binding with ligand after the generation, and prevent its further growth also shows the size distribution of zinc complex having arrangement of equispaced particles. The TEM images shows that zinc complex particles are not combined but are separated by equal interspace between the particles, which was confirmed by microscopy visualising under the higher resolution. The TEM images explains that the zinc complex are bounded with the ligand.

SEM images of Zinc(II) complex

SEM monographs in (Fig. 7) explains well dispersed, versatile and spherical shape of zinc complex when added to the ethanolic solution of ligand, does not change the shape of zinc complex particles but it increases the size of particles mostly in higher concentrations. The zinc complex particles are assembled into a very open and quasi- linear structure than a dense closely packed assembly.

TGA analysis of ligand & its Zinc(II) complex

The TGA Figure 8 indicate that the graphs ligand and its Zinc (II) complex begin to decompose at 276.93, 259°C, respectively. Comparison of the decomposition temperature of the compounds shows that zinc complex

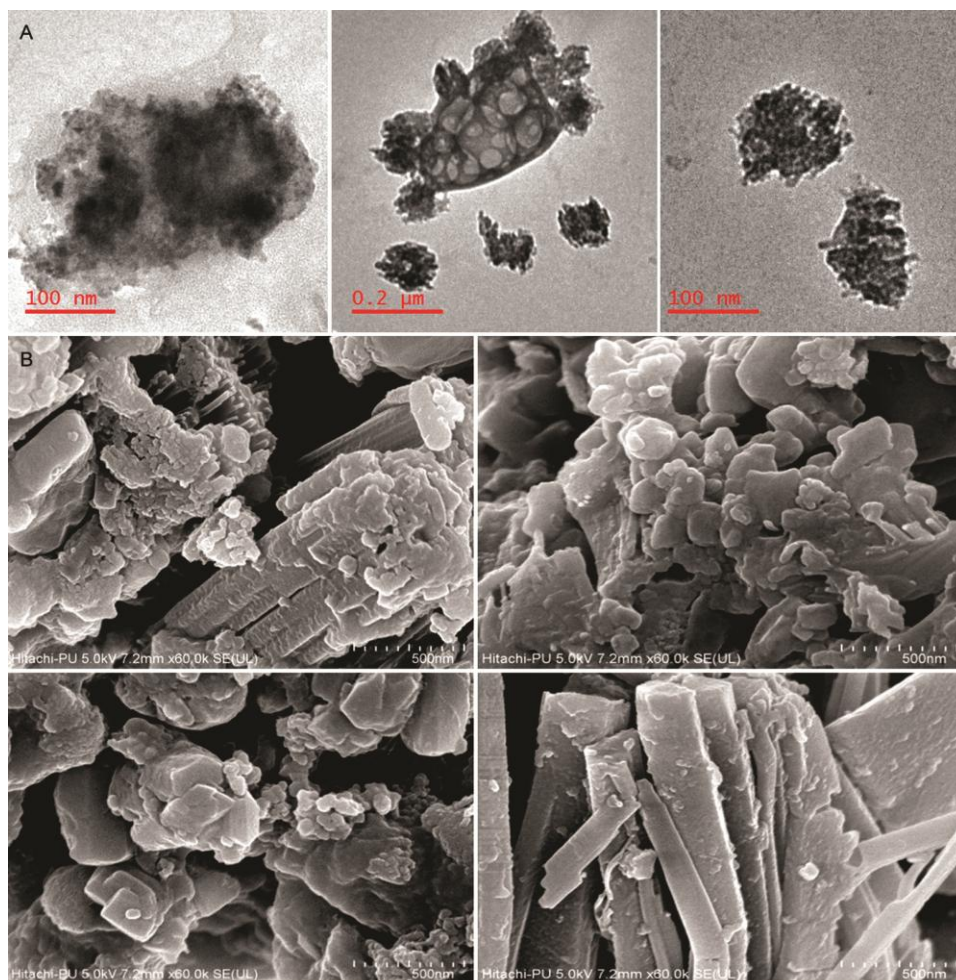


Fig.6 — (A) TEM Images; and (B) SEM Images of Zinc (II) Complex

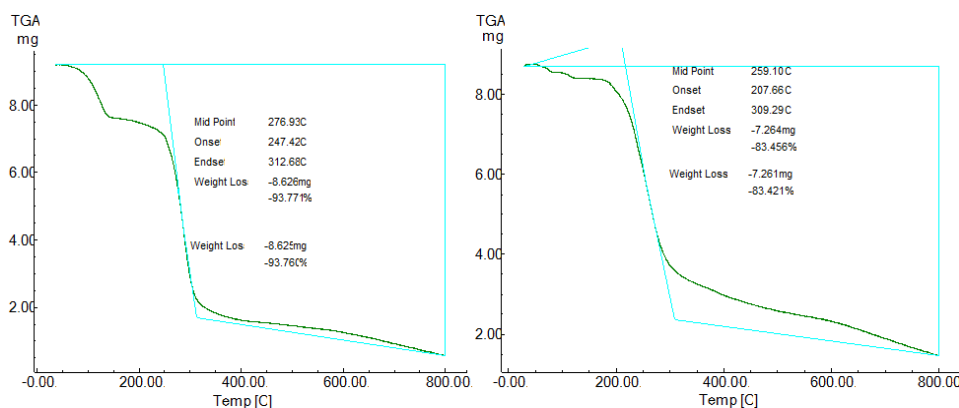


Fig. 7 — TGA Spectra of Ligand and its Zinc (II) Complex

decompose at higher temperature than its ligand. The TGA curve for zinc complex displays 8.626 mg weight loss within the temperature range of 150-800°C and exhibit a mass loss of 93.7%. The curve of ligand displays 7.26 mg weight loss within the temperature.

Antibacterial screening of ligand and its Zinc(II) complex

The antibacterial activity of hydrazone Schiff base ligand L and Zn(II) complex were examined using disc diffusion method and the results were summarized in (Tables 2 & 3 and Fig. 9). The results

Table 2 — Inhibition of standard drug Vancomycin-HCl against all test microbes

S. No.	Test Microbes	Diameter of Zone of Inhibition(in mm) at different drug concentration				
		50 µg/µL	25 µg/µL	12.5 µg/ µL	6.25 µg/µL	3.125 µg/µL
1	<i>E. Coli</i> (MTCC-1687)	11 mM	10 mM	Nil	Nil	Nil
2	<i>E. Faecalis</i> (MTCC-439)	30 mM	28 mM	25 mM	23 mM	20 mM
3	<i>S. aureus</i> (MTCC-737)	27 mM	26 mM	24 mM	22 mM	21 mM
4	M.R. <i>S. aureus</i> (Indigenous)	22 mM	21 mM	19 mM	19 mM	18 mM

Table 3 — Results of antibacterial activity of carbohydrazone Schiff base ligand (L₁) and its Zn(II) complex.

S. No.	Concentration (µg/µL) in Dichloromethane	<i>E. Coli</i> (MTCC-1687)		<i>S. aureus</i> (MTCC-737)		<i>E. Faecalis</i> (MTCC-439)	
		Ligand L ₁	Zn(II) complex	Ligand L ₁	Zn(II) complex	Ligand L ₁	Zn(II) complex
1	100 µg/µL	10	20	15	25	08	13
2	50 µg/µL	12	19	12	19	09	13
3	25 µg/µL	11	18	08	14	10	12
4	12.5 µg/µL	6.25	13	06	12	06	10
5	6.25 µg/µL	5.5	10	05	10	nil	nil

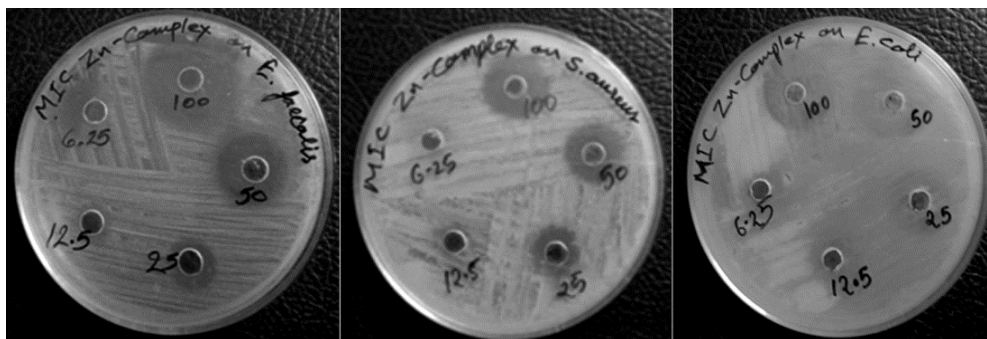


Fig. 8 — Anti bacterial activity of ligand and its Zinc (II) complexes

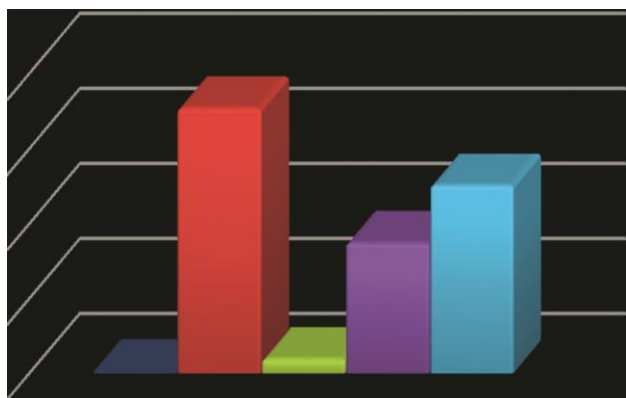


Fig. 9 — Graphical representation for antibacterial activity potential of ligand and its Zn(II) Complex in comparison to activity of standard vancomycin antibiotic

show that both ligand and its Zn(II) complex are considered nontoxic to gram positive and gram negative bacteria. Results show that Zn(II) complex is more reactive than its ligand(L); even the concentration was increased up to 6.25 µg/µL to

100 µg/µL the possible reason for this could be the absence of long hydrocarbon chains in both the structures of carbohydrazone and its Zn(II) complex (Fig. 9).

Molecular docking analysis

The molecular docking studies revealed that Zinc complex and ligand both got accessed into the active pockets of molecular targets and interacted with amino acids responsible for target inhibition. Although Zinc complex interacted with amino acid residues more efficiently in terms of binding affinity rather than ligand but Zn complex could not afford the hydrogen bond formation with active site residue in both targets whereas ligand could afford the formation of hydrogen bond with each target (Table 4). These results decipher here that significant binding affinity of zinc complex to topoisomerase II enzyme (Fig. 10) than that to DNA gyrase enzyme confirms that Zn complex (Fig. 11) is more effective against *S. aureus*.

Table 4 — Result of docking studies of Zn complexes and ligand

Name	Binding affinities (kcal/mol)with targets		Amino acids involved in the interactions		H-bond with distance	
	PDB=IJIJ	PDB=IKZN	PDB=IJIJ	PDB=IKZN	PDB=IJIJ	PDB=IKZN
Zn complex	-12.9	-11.2	Asp40, Thr42, Thr75, Gly83, Lys84, Ser85, Gly192, Asp195, Gln196, Val224 and Phe232	Met25, Asn46, Glu50, Ile78, His95, Glu117, His118, Val120 and Leu197	NIL	NIL
Ligand	-8.9	-7.9	Gly38, Ala39, His50, Leu70, Asp195, Gln196	Val43, Asn46, Glu50, Ile78, Ala96 and Val120	Asp195 (2.242 Å)	Asn46 (1.897Å)

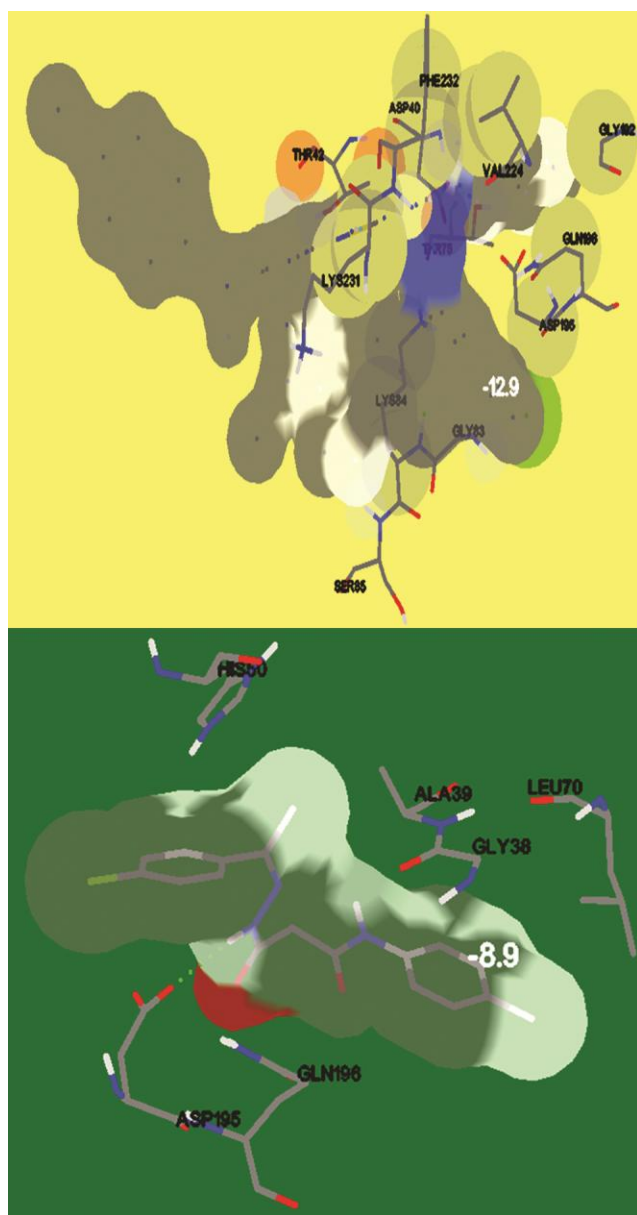


Fig.10 — A binding mode of (A) Zinc complex; and (B) ligand with topoisomerase II (3D model of interactions between ligand and target)

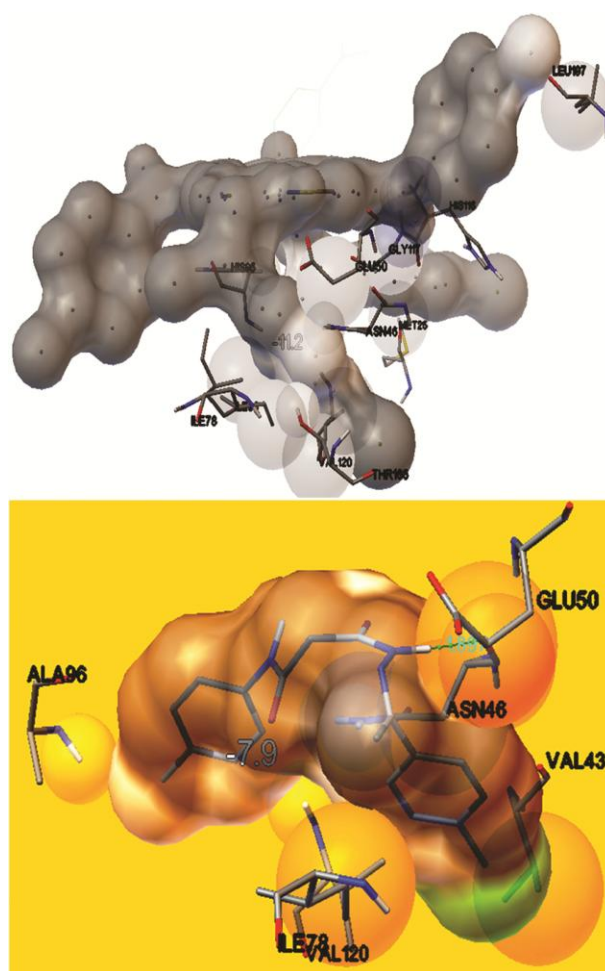


Fig.11 — A binding mode of (A) Zinc complex; and (B) ligand with DNA Gyrase (3D model of interactions between ligand and target)

Conclusion

In this study, synthesis, characterization, molecular docking and antibacterial activities of Bis-[(E)-3{2-(1-4 chlorophenyl)ethylidene}hydrazinyl]-N-(4-methylphenyl)-3-oxo propanamide Zinc (II) complex reported. The molecular structure of ligand and its Zn(II) complex are in agreement with the from

CHN elemental analysis and ¹HNMR spectroscopy results. In UV-Visible spectrum, the bathochromic shift of C=N wavelength absorption spectrum indicates the binding of azomethine nitrogen atoms from C=N to zinc²⁺ ion. From the result of antibacterial study, It is indicated that both ligand and its zinc complex showed the nontoxic behaviour towards both gram positive and gramnegative bacteria. Molecular docking studies also revealed, in terms of binding modes and binding energies, that zinc complex showed excellent binding to the receptor responsible for antibacterial effect.

Acknowledgement

Authors thank the management of ITM University, Gwalior for granting a mobility Grant in 2019. The authors are thankful to the SAIF Chandigarh for spectral analysis. Authors are also thankful to the multi-disciplinary laboratories of ITM University Gwalior for providing technical support.

Conflicts of interest

All authors declare no conflict of interest.

References

- Dutkiewicz G, Narayana B, Samshuddin S, Yathirajan HS & Kubicki M, Synthesis and crystal structures of two new Schiff base hydrazones derived from biphenyl-4-carbohydrazide. *J Chem Crystallogr*, 41(2011) 1442.
- Fita P, Luzina E, Dziembowska T, Kopec' D, Piatkowski P, Radzewicz Cz. & Grabowska A, Keto-enol tautomerism of two structurally related Schiff bases: Direct and indirect way of creation of the excited keto tautomer. *Chem Phy Lett*, 416 (2005) 305.
- Kelode SR & Mandlik PR, Synthesis, characterization, thermal and antibacterial studies of cobalt(II), nickel(II), copper(II) and zinc(II) complexes of hydrazone Schiff base. *Inter J Chem Pharm Sci*, 3 (2012) 30.
- Monfared HH, Pouralimardan O & Janiak C, Synthesis and spectral characterization of hydrazone Schiff bases derived from 2,4-dinitrophenylhydrazine. Crystal structure of salicylaldehyde-2,4-dinitrophenylhydrazine. *Z Naturforsch B*, 62 (2007) 717.
- Tay MG, Ngaini Z, Mohd Arif MA, Sarih NM, Khairul WM, Lau SP & Enggie E, Complexation of bis-2-(benzylideneamino) phenol to cobalt(II) and zinc(II), and their spectroscopic studies. *Borneo J Resour Sci Technol*, 3 (2013) 26.
- Siddiqi ZA, Shahid M, Khalid M & Kumar S, Anti microbial and SOD activities of novel transition metal ternary complexes of iminodiacetic acid containing α -diimine as auxiliary ligand. *Eur J Med Chem*, 44 (2009) 2517.
- Kumar LS, Prasad KS & Revanasiddappa HD, Synthesis, characterization, antioxidant, antimicrobial, DNA binding and cleavage studies of mononuclear Cu(II) and Co(II) complexes of 3-hydroxy-N'-(2-hydroxybenzylidene)-2-naphthohydrazide. *Eur J Chem*, 2 (2011) 394.
- Yaul SR, Yal AR, Pethe GB & Aswar AS, Synthesis and characterization of transition metal complexes with N, O-chelating hydrazone Schiff base ligand. *Am Eur J Sci Res*, 4 (2009) 229.
- Neelamma M, Rao PV & Anuradha GH, Synthesis and structural studies on transition metal complexes derived from 4-hydroxy-4-methyl-2-pentanone-1H-benzimidazol-2-yl-hydrazone. *E-J Chem*, 8 (2011) 29.
- Franks M, Gadzhieva A, Ghandhi L, Murrell D, Blake AJ, Davies ES, Lewis W, Moro F, McMaster J & Schröder M, Five coordinate M(II)-diphenolate [M=Zn(II), Ni(II), and Cu(II)] Schiff base complexes exhibiting metal-and ligand-based redox chemistry. *Inorg Chem*, 52 (2013) 660.
- Sztyk E, Wojtczak A, Surdykowski A & Gozdzikiewicz M, Five-coordinate zinc(II) complexes with optically active Schiff bases derived from (1R,2R)-(-)-cyclohexanediamine: X-ray structure and CP MAS NMR characterization of [cyclohexylenebis(5-chlorosalicylideneiminato) zinc(II)pyridine] and [cyclohexylenebis(5-bromosalicylideneiminato)zinc(II)pyridine]. *Inorg Chimica Acta*, 358 (2005) 467.
- Newman JM, Bear CA, Hambley TW & Freeman HC, Structure of bis(glycinato)zinc(II) monohydrate, a five-coordinate zinc(II) complex. *Acta Cryst*, 46 (1990) 44.
- Song XW, Gao XJ, Liu HX, Chen H, & Chen CN, Synthesis and characterization of a supra molecular assembly based on a pyridyl-functionalized [FeFe]-hydrogenase mimic and zinc tetraphenylporphyrin. *Inorg Chem Commun*, 70 (2016) 1.
- Che W, Yu T, Jin D, Ren X, Zhu D, Su Z & Bryce MR, A simple oxazoline as fluorescent sensor for Zn²⁺ in aqueous media. *Inorg Chem Commun*, 69 (2016) 89.
- Hall JB, Dobrovolskaia MA, Patri AK, McNeil SE, Characterization of nano particles for therapeutics. *Nanomed*, 2 (2007) 789.